

Research Article

**Spectroscopic Investigation, *ab initio* HF and DFT Calculations and Other Biomolecular Properties of 6-methylchromone-3-carbonitrile**J. Senthil kumar¹, S. Jeyavijayan^{2,*}, K. Gurushankar²¹PG & Research Department of Physics, Periyar E.V.R College (Autonomous), Tiruchirappalli, India.²Department of Physics, Kalasalingam University, Krishnankoil, Tamilnadu, India.*Corresponding author's E-mail: sjeyavijayan@gmail.com

Received: 17-10-2017; Revised: 03-11-2017; Accepted: 15-11-2017.

ABSTRACT

In this study, the experimental FTIR (4000–400 cm⁻¹) and FT-Raman spectra (3500-50 cm⁻¹) of 6-methylchromone-3-carbonitrile (MCCN) in solid phase have been recorded. The theoretical vibrational frequencies and optimized geometric parameters (bond lengths and bond angles) have been calculated by using *ab initio* HF and density functional theory (DFT/B3LYP) quantum chemical methods with 6-311++G(d,p) basis set. The assignments of the vibrational frequencies have been done by total energy distribution (TED) analysis. The theoretical optimized geometric parameters and vibrational frequencies have been found to be in good agreement with the corresponding experimental data, and with the results in the literature. The HOMO-LUMO energies have been investigated using the same theoretical calculations. MCCN exhibited good nonlinear optical activity and was much greater than that of urea. Molecular electrostatic potential (MEP) results predicted that the carbonitrile fragment of MCCN to be the most reactive site for both electrophilic and nucleophilic attack. In addition, Mulliken charges and thermodynamic properties were investigated using HF and DFT methods.

Keywords: FTIR, FT-Raman, MEP, 6-methylchromone-3-carbonitrile, DFT calculations.**INTRODUCTION**

Heterocyclic compounds and their derivatives which are important molecules in terms of pharmacological and biological properties are used extensively in the synthesis of various pharmacologically and biologically active compounds. Among them, Chromone constitute one of the major classes of naturally occurring compounds and interest in their chemistry continues unabated because of their usefulness as biologically active agent¹. Some of the biological activities attributed to chromone derivatives include cytotoxic (anticancer), neuroprotective, HIV-inhibitory, antimicrobial, antifungal and antioxidant activity²⁻⁴. In addition, Chromone and its derivatives are widely distributed in plant life, mostly as pigments in plant leaves and flowers. Moreover, the pharmacological activities of many chromone derivatives such as anti-inflammatory, anti-viral and anti-neoplastic activities have been extensively investigated^{5, 6}. Heterocyclic ring fused on substituted chromones has become attractive targets in organic synthesis because of their significance in biological systems and wide range of occurrence in natural products⁷. They have good pharmacological activities such as coronary, spasmolytic and bronchodilatory activities and are useful in the treatment of asthma⁸. Also, chromones have drawn great attention from cosmetic, anti-nutrocentical and pharmaceutical industries with anti-inflammation, anti-ulcer, tyrosine's inhibition, skin protection and laxative effect⁹. In recent years considerable interest has arisen in the chemistry of chromones and its derivatives, where as spectroscopic and structural studies are limited. To evaluate the relationship between biological activity and molecular

structure, the knowledge of their electronic structure and spectral properties are particularly important. In view of the biological activities associated with the chromone derivatives and its related importance in pharmaceutical industries, the spectral characteristics of 6-methyl chromone-3-carbonitrile (MCCN) utilizing the FTIR and FT-Raman spectra is investigated in the present work. The purpose of this present study is to record and analysis the vibrational spectra of the molecule completely in the solid state and also carried out to identify NLO property (first hyperpolarizability), HOMO–LUMO energy gap, atomic charge, MEP and other molecular properties. All these investigation have been done on the optimized structure of the molecule by using the *ab initio* Hartree-Fock (HF) and Becke's three-parameter-Lee-Yang-Parr (B3LYP) methods with 6-311++G(d,p) basis set.

MATERIALS AND METHODS

The fine polycrystalline sample of MCCN was purchased from the Aldrich Chemical Company, USA which is of spectroscopic grade and used as such without any further purification to record FTIR and FT-Raman spectra. The FTIR spectrum of MCCN have been recorded in solid state in the region 4000-400 cm⁻¹ using BRUKER IFS-66V FTIR spectrometer with scans of spectral width 2.0 cm⁻¹. The FT-Raman spectrum of MCCN was recorded in the FT-Raman BRUKER IFS 100/s model equipped with Nd: YAG laser source operating at 150mW power continuously with 1064 nm of spectral width 2 cm⁻¹. The frequencies of all sharp bands are accurate to ±4 cm⁻¹.

Computational Details

The molecular structure of the title compound is computed by performing both *ab initio* HF and DFT



(B3LYP) with 6-311++G(d,p) basis set calculations. The optimized structural parameters are used in the vibrational frequency calculations at HF and DFT levels. All the computation has been done by adding polarization function p and diffuse function d using GAUSSIAN 09W program package¹⁰. By combining the results of GAUSSVIEW program¹¹ with symmetry considerations, vibrational frequency assignments were made with high degree of confidence. The total energy distribution (TED) is computed for quantum chemically calculated vibrational frequencies using MOLVIB program¹². Further, Investigation has been carried out to identify HOMO–LUMO energy gap, NLO (first hyperpolarizability)

properties, MEP, Mullikan atomic charges for the optimized molecular structure.

RESULTS AND DISCUSSION

Molecular geometry

The molecular structure of the MCCN belongs to C_1 point group symmetry. The optimized molecular structure of the title molecule is shown in Fig. 1. The minimum energy of MCCN was calculated by structure optimization at HF and B3LYP/6-311++G(d,p) are -624.94418786 a.u. and -628.73203789 a.u., respectively. The optimized bond lengths and bond angles of MCCN which are calculated by using same methods and basis sets are listed in Table 1.

Table 1: Optimized geometrical parameters of 6-methylchromone-3-carbonitrile obtained by HF and B3LYP using 6-311++G(d, p) basis set.

Bond length	Value (Å)		Expt ^a	Bond angle	Value (°)		Expt ^a
	HF	B3LYP			HF	B3LYP	
O1-C2	1.3158	1.3348	1.348	C2-O1-C9	119.7453	119.1788	118.54
O1-C9	1.3619	1.3802	1.377	O1-C2-C3	124.6304	124.5251	124.97
C2-C3	1.3373	1.3576	1.347	O1-C2-H11	112.3614	111.8953	117.5
C2-H11	1.0729	1.0823	0.95	C3-C2-H11	123.0081	123.5796	117.5
C4-C10	1.4798	1.4801	1.476	C2-C3-C4	120.2642	120.7817	120.15
C3-C4	1.4762	1.4807	1.464	C3-C4-C10	112.9357	113.1728	-
C3-C12	1.4354	1.4250	-	C3-C4-O14	123.7211	123.2800	123.61
C4-O14	1.1898	1.2179	1.233	C6-C5-H15	121.0742	121.1940	119.7
C5-C6	1.3741	1.3876	1.381	C10-C5-H15	117.5565	117.2860	119.7
C5-C10	1.4001	1.4042	1.402	C5-C6-C7	117.9224	118.1669	116.29
C5-H15	1.0741	1.0839	0.95	C5-C6-C16	121.8222	121.5321	120.01
C6-C7	1.4044	1.4101	1.403	C7-C6-C16	120.1954	120.3009	122.62
C6-C16	1.5099	1.5086	1.506	C6-C7-C8	121.8878	121.7131	120.68
C7-C8	1.3721	1.3842	1.374	C6-C7-H20	119.2591	119.3299	119.7
C7-H20	1.0763	1.0850	0.95	C8-C7-H20	118.8531	118.9570	119.7
C8-C9	1.3891	1.3938	1.395	C7-C8-C9	118.657	118.6600	118.51
C8-H21	1.0738	1.0829	0.95	C7-C8-H21	121.795	121.8044	120.7
C9-C10	1.3779	1.3952	1.391	C9-C8-H21	119.5479	119.5356	120.7
C12-N13	1.1302	1.1550	-	O1-C9-C8	116.8682	116.7565	-

^aExperimental values are taken from Ref. ¹³.

The results show that the B3LYP/6-311++G(d,p) method is in good agreement with the experimental values¹³ than the HF method. As a result of experimental findings and our calculations C4–O14 bonds show typical double-bond characteristics whereas O1–C2, O1–C9 bonds show single-bond characteristics. The C4–O14 bond length is relatively shorter due to the electron-withdrawing effect depending on the presence of the carbonyl group linked to this bond. The bond lengths C4–C10, C3–C4, C6–C7 and C8–C9 are

longer than the bond lengths C2–C3, C5–C6, C5–C10, C7–C8, C9–C10 and angles slightly out of the regular hexagonal structure. These distortions are explained in terms of the change in hybridisation affected by the substituent at the carbon site to which it is appended. The bond angles O1–C2–C3 and C6–C7–C8 are increases and the angles C3–C4–C10, C2–C3–C4 and C5–C6–C7 are deviates from typical hexagonal angle of 120°. This is because of the effect of substitution of oxygen atom



attached to C4 of the ring, nitrile group attached to C3 and methyl group attached to C6 of the ring. It can be seen that there are some deviations in the computed geometrical parameters from those reported in the related XRD data, and these differences are probably due to the fact that the theoretically calculated result is obtained from isolated molecule in gaseous phase while the experimental results are from molecule in solid state.

Vibrational assignments

The observed vibrational assignments and analysis of MCCN are discussed in terms of infrared and Raman

bands. The molecule consists of 21 atoms and expected to have 57 normal modes of vibrations of the same A species under C_1 symmetry. These modes are found to be IR and Raman active suggesting that the molecule possesses a non-centrosymmetric structure, which recommends the title compound for non-linear optical applications. The FTIR and FT-Raman spectra of MCCN are shown in Fig. 2. The observed and calculated frequencies using HF and B3LYP methods with 6-311++G(d,p) basis set along with their force constants and probable assignments for MCCN are given in Table 2.

Table 2: Assignment of fundamental vibrational modes of 6-methylchromone-3-carbonitrile based on SQM force field calculations using scaled B3LYP/6-31+G (d,p) and HF/6-31+G(d,p) force fields.

Species C_1	Observed Frequencies (cm^{-1})		Calculated Frequencies (cm^{-1})						Assignment (% of TED)
			HF/6-311++G(d, p)			B3LYP/6-311++G(d, p)			
	FTIR	FT-Raman	Unscaled	Scaled	Force Constants	Unscaled	Scaled	Force Constants	
A	3097(w)	3102(ms)	3388	3083	7.4280	3217	3088	6.6769	vCH(98)
A	-	3090(ms)	3362	3059	7.3004	3200	3072	6.6029	vCH(96)
A	-	3086(ms)	3360	3058	7.2731	3189	3061	6.5400	vCH(94)
A	3074(vs)	3072(vs)	3325	3026	7.1105	3168	3041	6.4449	vCH(92)
A	2990(ms)	-	3252	2959	6.8656	3113	2988	6.2844	CH ₃ ss(90)
A	2950(w)	-	3220	2930	6.7340	3077	2954	6.1423	CH ₃ ips(91)
A	2860(w)	-	3169	2884	6.1431	3028	2907	5.6077	CH ₃ ops(90)
A	2232(vs)	2232(vs)	2589	2356	50.1180	2340	2246	40.9088	vC≡N(88)
A	1701(ms)	1708(s)	1944	1769	28.9662	1730	1661	22.4308	vC=O(85)
A	-	1668(vs)	1810	1647	11.6193	1653	1587	10.4666	vCC(82)
A	1654(vs)	-	1806	1643	12.3955	1644	1578	10.0651	vCC(84)
A	-	1635(w)	1753	1595	11.5670	1605	1541	9.2980	vCC(83)
A	1613(ms)	-	1644	1496	4.7388	1510	1450	3.9184	vCC(80)
A	-	1609(w)	1620	1474	1.9733	1500	1440	1.6083	vCC(78)
A	-	1572(w)	1604	1460	1.5828	1487	1428	1.3598	vCC(79)
A	1568(w)	-	1577	1435	4.1197	1449	1391	1.8893	vCC(81)
A	-	1525(w)	1542	1403	1.7592	1420	1363	1.4793	vCC(76)
A	1478(vs)	-	1508	1372	3.4235	1380	1325	2.2026	vCC(75)
A	1462(w)	-	1461	1330	2.4760	1366	1311	9.2957	vCC(78)
A	1448(w)	-	1405	1279	2.8434	1336	1283	2.3187	vC-O(74)
A	1434(s)	1432(s)	1387	1262	2.8062	1288	1236	1.6522	vC-O(73)
A	1422(ms)	-	1314	1196	2.4340	1256	1206	6.3538	vCC(75)
A	-	1372(w)	1301	1184	3.5158	1212	1164	2.5048	CH ₃ sb(76)
A	-	1270(ms)	1279	1164	2.5778	1195	1147	2.3551	CH ₃ ipb(74)
A	1237(s)	1239(w)	1277	1162	2.2629	1161	1115	1.2810	CH ₃ opb(72)
A	-	1192(w)	1202	1094	2.1357	1124	1079	2.1374	bCH(70)
A	1185(vw)	-	1168	1063	1.2359	1067	1024	1.0320	bCH(68)
A	1136(vw)	1137(vw)	1102	1003	1.3355	1034	993	1.1121	bCH(71)
A	-	1103(w)	1098	999	0.9556	983	944	0.7631	bCH(69)



A	-	1063(vw)	1085	987	0.9838	979	940	1.4127	CH ₃ ipr(70)
A	1045(ms)	1048(w)	1047	953	1.7882	937	900	0.7292	CH ₃ opr(72)
A	958(s)	956(vw)	1024	932	0.8447	931	894	0.6957	bCC(71)
A	952(s)	-	953	867	3.0662	886	851	2.6836	bCC(70)
A	-	940(w)	925	842	0.7341	835	802	0.5832	R1 trigd(72)
A	-	891(w)	877	798	2.7318	802	770	2.2888	R2 trigd(74)
A	881(vs)	-	832	757	2.9320	776	745	2.5242	R1symd(68)
A	-	795(s)	779	709	1.6028	728	699	1.7481	R2symd(69)
A	771(vs)	-	776	706	2.0377	713	684	1.3793	R1asymd(69)
A	-	739(w)	731	665	2.2745	686	659	2.0462	R2asymd(66)
A	-	730(w)	694	632	2.4846	639	613	2.0917	ωCH(62)
A	719(ms)	-	616	561	1.0270	565	542	0.8098	ωCH(64)
A	-	680(vw)	583	531	0.8812	533	512	0.7736	ωCH(61)
A	670(vw)	-	559	509	1.3919	523	502	1.1935	ωCH(63)
A	624(ms)	-	520	473	1.0609	480	461	0.8589	tR1trigd(60)
A	554(ms)	-	512	466	0.6811	471	452	0.6383	tR2trigd(59)
A	-	520(vw)	467	425	1.0902	429	412	0.9923	tR1symd(62)
A	514(vw)	-	452	411	0.4072	419	402	0.3527	tR2symd(63)
A	-	501(vw)	392	357	0.6395	370	355	0.6088	bCN(68)
A	-	488(vw)	388	353	0.3970	364	349	0.3322	tR1asymd(65)
A	467(ms)	-	342	311	0.2629	313	300	0.2203	tR2asymd(64)
A	-	342(w)	247	225	0.1703	231	222	0.1496	ωCC(62)
A	-	320(vw)	237	216	0.3344	222	213	0.2928	ωCC(61)
A	-	313(vw)	177	161	0.0867	162	156	0.0739	bCO(65)
A	-	288(vw)	140	127	0.1031	127	122	0.0876	ωCN(62)
A	-	191(vw)	130	118	0.0459	117	112	0.0365	ωCO(60)
A	-	182(vw)	76	69	0.0037	58	56	0.0041	CH ₃ twist(59)
A	-	103(vw)	57	52	0.0132	51	49	0.0027	Butterfly(56)

Abbreviations: *w*-weak, *s*-strong, *ms*-medium strong, *vw*-very weak, *vs*-very strong, *R*-ring, *b*-bending, *v*-stretching, *symd*-symmetric deformation, *ω*-out-of-plane bending, *asymd*-antisymmetric deformation, *trigd*-trigonal deformation, *ss*-symmetric stretching, *ips*-in-plane stretching, *sb*-symmetric bending, *ipb*-in-plane-bending, *ipr*-in-plane-rocking, *ops*-out-of-plane stretching, *opb*-out-of-plane bending, *opr*-out-of-plane rocking, *t*-torsion, *twist* - twisting.

The calculated frequencies are slightly higher than the observed values for the majority of the normal modes. Two factors may be responsible for the discrepancies between the experimental and computed spectra of this compound. The first is caused by the environment and the second reason for these discrepancies is the fact that the experimental value is an anharmonic frequency while the calculated value is a harmonic frequency. Therefore, in order to improve the calculated values in agreement with the experimental ones, it is necessary to scale down the calculated harmonic frequencies. A better agreement between the computed and experimental frequencies can be obtained by using scale factor¹⁴ of 0.91 and 0.96 for HF and B3LYP methods, respectively. The scaled frequencies are also presented in Table 2.

C-H vibrations

The title compound is fused with an aromatic and hetero aromatic ring system in which one of the ring is benzene. Hence, the molecular structure of the title compound shows the C-H stretching vibrations. The C-H stretching vibration of benzene derivatives generally appear in the region 3000–3100 cm⁻¹, which is the characteristic region for ready identification of C-H stretching vibration¹⁵. Accordingly, in the present investigation, the C-H stretching vibrations of MCCN are observed at 3097, 3074 cm⁻¹ in the FTIR spectrum and 3102, 3090, 3086, 3072 cm⁻¹ in FT-Raman spectrum. These modes are supported by the literature¹⁵ in addition to the TED output (almost 100%). The C-H in-plane bending frequencies appear in the range 1000–1300 cm⁻¹ and are very useful for characterization purpose for MCCN. The C-H in-plane



bending vibrations of MCCN appeared at 1185, 1136 cm^{-1} and 1137, 1103 cm^{-1} in the FTIR and FT-Raman spectra, respectively. The C-H out-of-plane bending vibrations¹⁶ are strongly coupled vibrations and occur in the region

900-667 cm^{-1} . The aromatic C-H out-of-plane bending vibrations of MCCN are assigned to the bands observed at 719, 670 cm^{-1} and 730, 680 cm^{-1} in the FTIR and FT-Raman spectra, respectively.

Table 3: The thermodynamic parameters of 6-methylchromone-3-carbonitrile.

Parameters	Method/Basis set	
	HF/6-311++G(d,p)	B3LYP/6-311++G(d,p)
Optimized global minimum Energy (Hartrees)	-624.94418786	-628.73203789
Total energy(thermal), E_{total} (kcal mol ⁻¹)	109.731	103.097
Heat capacity, C_v (cal mol ⁻¹ K ⁻¹)	40.351	43.271
Entropy, S (cal mol ⁻¹ K ⁻¹)		
<i>Total</i>	102.802	106.138
<i>Translational</i>	41.553	41.553
<i>Rotational</i>	31.394	31.437
<i>Vibrational</i>	29.855	33.148
Vibrational energy, E_{vib} (kcal mol ⁻¹)	107.953	101.320
Zero point vibrational energy, (kcal mol ⁻¹)	103.02562	95.93462
Rotational constants (GHz)		
<i>A</i>	1.71370	1.67196
<i>B</i>	0.46030	0.45703
<i>C</i>	0.36365	0.35972
Dipole moment (Debye)		
μ_x	-6.4947	-6.5310
μ_y	4.6771	4.4425
μ_z	0.0000	0.0001
μ_{total}	8.0035	7.8987

Methyl group vibrations

The MCCN molecule has one methyl groups in the sixth position. For the assignments of CH₃ group frequencies, basically nine fundamentals can be associated to each CH₃ group namely CH₃ ss-symmetric stretching; CH₃ ips-in-plane stretching (i.e., in-plane hydrogen stretching modes); CH₃ ipb-in-plane bending (i.e., hydrogen deformation modes); CH₃ sb-symmetric bending; CH₃ ipr-in-plane rocking; CH₃ opr-out-of-plane rocking; CH₃ ops-out-of-plane stretching; CH₃ opb-out-of-plane bending modes. The stretching in CH₃ occurs at lower frequencies than those of aromatic ring (3000–3100 cm^{-1}). The CH₃ stretching¹⁷ is expected around 2900–3000 cm^{-1} , the in-plane deformations around 1370–1450 cm^{-1} and the rocking around 990–1040 cm^{-1} . For MCCN, the CH₃ symmetric stretching frequency is observed at 2990 cm^{-1} in the FTIR spectrum. The CH₃ in-plane and out-of-plane stretching vibrations are observed at 2950 and 2860 cm^{-1} in IR spectrum. For the methyl substituted benzene derivatives¹⁸, the in-plane and symmetric bending deformation vibrations of methyl groups normally appear in the region 1440–1465 cm^{-1} and 1370–1390 cm^{-1} , respectively. In the present work, the frequency of 1372 and 1270 cm^{-1} in FT-Raman are assigned to the symmetric bending and in-plane bending modes of CH₃ group. The MCCN appear as independent vibrations in 1063 and 1048 cm^{-1} in FT-Raman have been assigned to the CH₃ in-

plane rocking and out-of plane rocking, respectively. The IR counterpart of CH₃ out-of plane rocking is found at 1045 cm^{-1} . All these vibrations coincide very well with the calculated DFT frequencies. The CH₃ torsional mode is expected below 400 cm^{-1} , the FT-Raman band at 182 cm^{-1} in MCCN is assigned to this mode.

C≡N vibration

Unsaturated and aromatic nitriles, in which the double bond or ring is adjacent to C≡N group, absorb more strongly in infrared region than saturated compounds, and the related band occurs at somewhat lower frequency around 2230 cm^{-1} . The characteristic wave number of C≡N stretching vibration¹⁹ is observed in the region 2240–2220 cm^{-1} . In the present study, the FTIR and Raman bands at 2232 cm^{-1} is assigned to the stretching of C≡N group, and the corresponding force constant contribute 88% to the TED. The C≡N in-plane and out-of-plane bending modes of MCCN are also listed in Table 2.

Carbonyl vibrations

Almost all carbonyl compounds²⁰ have a very intense and narrow peak in the range of 1800–1600 cm^{-1} or in other words the carbonyl stretching frequency has been most extensively studied by infrared spectroscopy. Chromone



have two characteristic strong absorption bands arising from C=O and C–O stretching vibrations. The intense C=O stretching vibrations occurs at higher frequencies than that normal ketones. In our present study, the bands at 1701 and 1708 cm^{-1} in FTIR and Raman, respectively are assigned to the C=O vibration of MCCN and the corresponding DFT computed mode at 1730 cm^{-1} is in good agreement with the observed as well as related work²⁰. The C=O in-plane and out-of-plane bending modes of MCCN are also confirmed by their TED values.

HOMO, LUMO analysis

The highest occupied molecular orbitals (HOMOs) and the lowest-lying unoccupied molecular orbitals (LUMOs) are named as frontier molecular orbitals (FMOs). The FMOs play an important role in the electric and optical properties, as well as in UV–Vis spectra and chemical reactions²¹. The atomic orbital HOMO and LUMO compositions of the frontier molecular orbital for MCCN computed at the B3LYP/6-311++G(d,p) are shown in Fig. 3. The calculations indicate that the title compound have 48 occupied MOs. The HOMO-LUMO energy gap for MCCN is found to be 4.803 eV. The decrease in energy gap between HOMO and LUMO facilitates the molecular charge transfer which makes the material to be NLO active. The LUMO: of π nature, (i.e. benzene ring) is delocalized over the whole C-C bond. By contrast, the HOMO is located over nitrile and methyl groups; consequently the HOMO \rightarrow LUMO transition implies an electron density transfer to C-C and C-O bonds of the ring from nitrile and methyl groups. Moreover, these orbitals significantly overlap in their position of the ring for MCCN. The LUMO as an electron acceptor represents the ability to obtain an electron, and HOMO represents the ability to donate an electron.

Mulliken population analysis

Mulliken atomic charge calculation²² has an important role in the application of quantum chemical calculation to molecular system due to the change in dipole moment, polarizability, electronic structure, and much more properties of molecular systems. The total atomic charges of MCCN obtained by HF and B3LYP methods with 6-311++G(d,p) basis set are graphically represented in Fig. 4 and it gives us information about the charge shifts related to MCCN. The charge distribution on the molecule has an important influence on the vibrational spectra. More charge density was found at C3, C9 and C10 than that of other ring carbon atoms. The high positive charge at C6 and C10 is due to the effect of electron releasing methyl group and aromatic oxygen attached with these atoms. The electron donating character of the nitrile group in the title compound is demonstrated by a increase in electron density on C3 atom. From the result it is clear that the substitution of nitrile and methyl groups in the aromatic ring leads to a redistribution of electron density.

Electrostatic potential, total electron density and molecular electrostatic potential

The electrostatic potential has been used primarily for predicting sites and relative reactivities towards electrophilic attack, and in studies of biological recognition and hydrogen bonding interactions²³. To predict reactive sites for electrophilic and nucleophilic attack for the investigated molecule, the MEP at the B3LYP/6-31+G(d,p) optimized geometry was calculated. In the present study, the electrostatic potential (ESP), electron density (ED) and the molecular electrostatic potential (MEP) map figures for MCCN are shown in Fig. 5. The ED plots for the title molecule show a uniform distribution. However, the ESP figures shows that the negative potential is localized more over the nitrile, methyl and oxygen atom of carbonyl groups and is reflected as a yellowish blob, the positive ESP is localized on the rest of the molecule. This result is expected, because ESP correlates with electro negativity and partial charges. The different values of the electrostatic potential at the surface are represented by different colours. In general, potential increases in the order red < orange < yellow < green < blue. In the Fig. 5, the negative (red and yellow) regions of the MEP are related to electrophilic reactivity and the positive (blue) regions to nucleophilic reactivity. As can be seen from the figure and the computed results, the MEP map shows that the negative potential sites are in double bonded oxygen atom and nitrogen in the nitrile group and the positive region is over the hydrogen atom in the ring. From these results, the H atoms in the ring indicate the strongest attraction and oxygen and nitrogen atoms indicate the strongest repulsion. The region of all hydrogen atoms in the methyl group are indicated by green, since they are neutral. These sites give information about the region from where the compound can have intermolecular interactions. Thus, it would be predicted that the MCCN molecule will be the most reactive site for both electrophilic and nucleophilic attack.

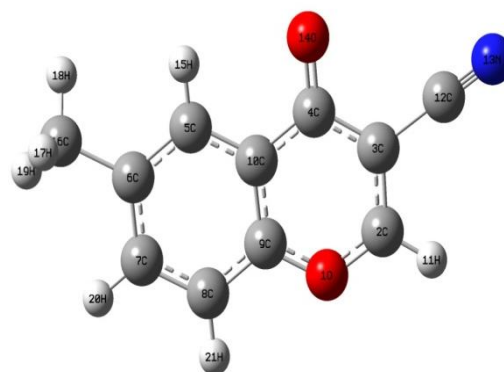


Figure 1: Molecular structure of 6-methylchromone-3-carbonitrile.

Other molecular properties

Normally, the thermo dynamical analysis on aromatic compound is very important since they provide the necessary information regarding the chemical reactivity.

On the basis of vibrational analysis at the HF and B3LYP methods with 6-31+G(d,p) basis set, the standard statistical thermodynamic functions: heat capacity, zero point energy, entropy of MCCN have been calculated and are presented in Table 3. The difference in the values calculated by both the methods is only marginal. The variation in the ZPVE seems to be significant. Dipole moment reflects the molecular charge distribution and is given as a vector in three dimensions. Therefore, it can be used as descriptor to depict the charge movement across the molecule. Direction of the dipole moment vector in a molecule depends on the centres of positive and negative charges. The total dipole moment of MCCN determined by HF and B3LYP methods using 6-311++G(d,p) basis set are 8.0035 and 7.8987 Debye, respectively. The total energy and the change in the total entropy of the compound at room temperature are also presented. All the thermodynamic data are helpful for the further study on the MCCN. They can be used to compute the other thermodynamic energies and estimate directions of chemical reactions.

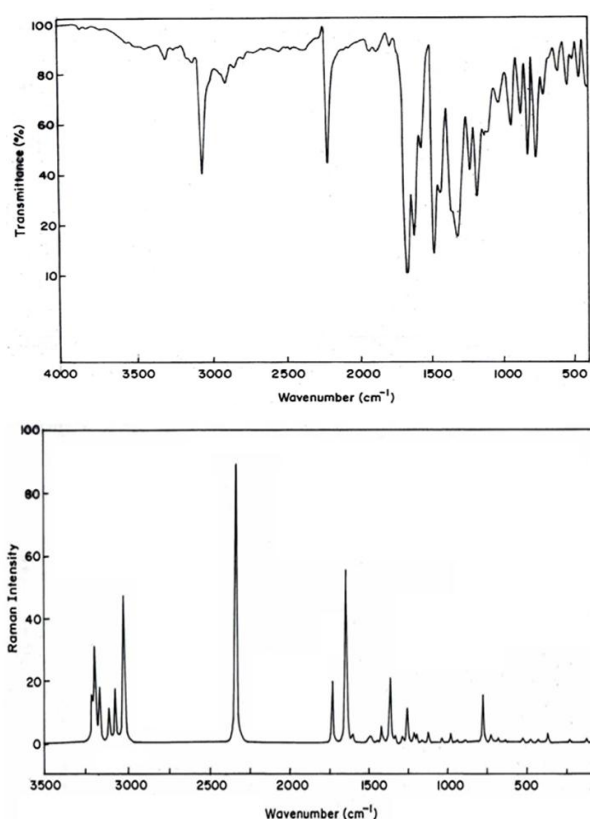


Figure 2: FTIR and FT-Raman spectra of 6-methylchromone-3-carbonitrile.

First hyperpolarize ability and NLO activity

Analysis of organic molecules having conjugated π -electron systems and large hyperpolarize ability using IR and Raman spectroscopy has evolved as a subject of research. The potential application of the title molecule in the field of non-linear optics demands the investigation of its structural and bonding features contributing to the hyperpolarizability enhancement by analyzing the

vibrational modes using IR and Raman spectroscopy. The B3LYP/6-311++G(d,p) method has been used for the prediction of first hyperpolarizability. The total static dipole moment μ , the average linear polarizability $\bar{\alpha}$, the anisotropy of the polarizability $\Delta\alpha$, and the first hyperpolarizability β can be calculated by using the following Equations²⁴:

$$\bar{\alpha} = \frac{1}{3}(\alpha_{xx} + \alpha_{yy} + \alpha_{zz})$$

$$\Delta\alpha = \frac{1}{\sqrt{2}} \left[(\alpha_{xx} - \alpha_{yy})^2 + (\alpha_{yy} - \alpha_{zz})^2 + (\alpha_{zz} - \alpha_{xx})^2 + 6\alpha_{xx}^2 \right]^{1/2}$$

$$\mu = (\mu_x^2 + \mu_y^2 + \mu_z^2)^{1/2}$$

$$\beta = [(\beta_{xxx} + \beta_{yy} + \beta_{zz})^2 + (\beta_{yyy} + \beta_{xx} + \beta_{zz})^2 + (\beta_{zz} + \beta_{xx} + \beta_{yy})^2]^{1/2}$$

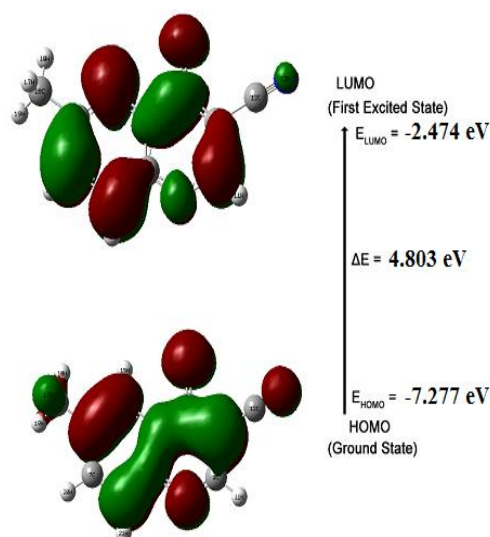


Figure 3: Frontier molecular orbital for 6-methylchromone-3-carbonitrile.

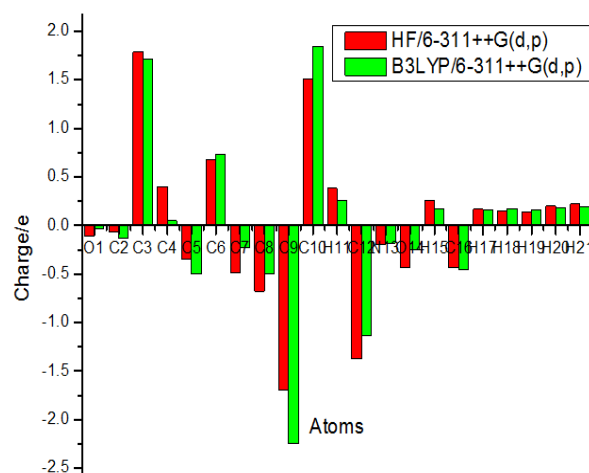
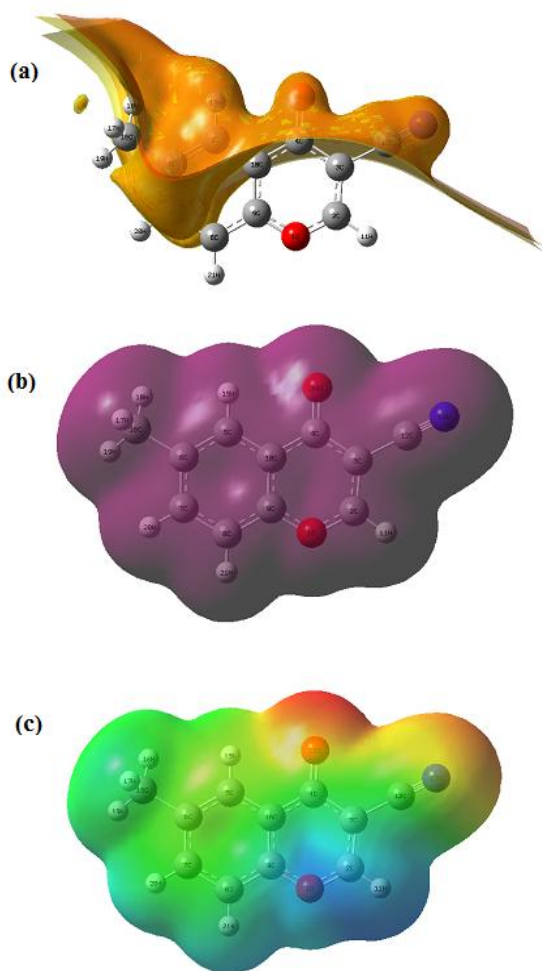


Figure 4: Mulliken's plot for 6-methylchromone-3-carbonitrile.

The calculated values of total static dipole moment μ , the average linear polarizability $\bar{\alpha}$, the anisotropy of the polarizability $\Delta\alpha$, and the first hyperpolarizability β using the DFT-B3LYP/6-311++G(d,p) method are 7.8987 Debye, 20.79 Å³, 24.38 Å³ and 4.052×10⁻³⁰ e.s.u.⁻¹, respectively.

The values of μ , $\bar{\alpha}$ and β obtained by Sun *et al.*²⁵ with the B3LYP method for urea are 1.373 Debye, 3.831 Å³ and 0.3729×10⁻³⁰ e.s.u.⁻¹, respectively. The first hyperpolarizability of MCCN molecule is 10 times greater than that of urea. The large value of hyperpolarizability, β_0 which is a measure of the non-linear optical activity of the molecular system, is associated with the intramolecular charge transfer, resulting from the electron could movement through π conjugated frame work from electron donor to electron acceptor groups. So, we conclude that the title compound is an attractive object



for future studies of nonlinear optical properties.

Figure 5: (a) Electrostatic potential (ESP); (b) electron density (ED) and (c) the molecular electrostatic potential (MEP) map for 6-methylchromone-3-carbonitrile.

CONCLUSION

The molecular structural parameters and fundamental vibrational frequencies of 6-methylchromone-3-carbonitrile have been obtained from *ab initio* HF and DFT calculations. The effect of methyl and nitrile group substituents on vibrational frequencies is analysed in detail. The assignments of most of the fundamentals provided in the present work are believed to be unambiguous. The TED calculation about the normal modes of vibration provides a strong support for the frequency assignment. The calculated first order

hyperpolarizability was found to be 4.052×10⁻³⁰ e.s.u.⁻¹, which is 10 times greater than reported in literature for urea. The HOMO and LUMO energy gap shows that the charge transfer occur within the molecule, which are responsible for the bioactive property of the molecule. The MEP map predicts the reactive sites for electrophilic and nucleophilic attack the molecule and the results are discussed. Furthermore, the thermodynamic and Mulliken charge analysis of the compound have been calculated in order to get insight into the compound.

REFERENCES

1. Miao H, Yang Z, Regiospecific Carbonylative Annulation of Iodophenol Acetates and Acetylenes To Construct the Flavones by a New Catalyst of Palladium–Thiourea–dppp Complex, *Org. Lett.*, 2, 2000, 1765-1768.
2. Larget R, Lockhart B, Renard P, Largeram M, A convenient extension of the Wessely–Moser rearrangement for the synthesis of substituted alkyl aminoflavones as neuroprotective agents in vitro, *Biorg. Med. Chem. Lett.*, 10, 2000, 835-838.
3. Groweiss A, Cardellins JH, Boyd MR, HIV-Inhibitory prenylated xanthenes and flavones from *Maclura tinctoria*, *J. Nat. Prod.*, 63, 2000, 1537-1539.
4. Pietta PG, Flavonoids as antioxidants, *J. Nat. Prod.* 63, 2000, 1035-1042.
5. De Meyer N, Haemers A, Mishra L, Pandey HK, Pieters LAC, Berghe DAV, Vlietinck AJ, 4'-Hydroxy-3-methoxyflavones with potent anticoronavirus activity, *J. Med. Chem.* 34, 1991, 736-746.
6. Beutle JA, Cardellina JH, Lin CY, Hamel E, Cragg GM, Boyd MR, Centaureidin, a cytotoxic flavone from *Polymnia fruticosa*, inhibits tubulin polymerization, *Biorg. Med. Chem. Lett.* 3, 1993, 581-584.
7. Youssef NS, Separation and Characterization of New Transition Metal Complexes of some Chromone Derivatives, *Asian J. Chem.*, 11, 1999, 1407-1417.
8. Ellis GP, Shaw D, Benzopyrones. Part VIII. Mono- and di-tetrazol-5-ylchromones. The infrared cyano-absorption of some 4-oxochromencarbonitriles, *J. Chem. Soc. Perkin Trans.*, 1, 1972, 779-783.
9. Arjunan V, Subramanian S, Mohan S, FTIR and FTR spectral studies of 2-amino-6-bromo-3-formylchromone, *Spectrochim. Acta*, 60A, 2004, 995-1000.
10. Frisch MJ, Trucks GW, Schlegel HB, Scuseria GE, Robb MA, Cheeseman JR, Scalmani G, Barone V, Mennucci B, Petersson GA, Nakatsuji H, Caricato M, Li X, Hratchian HP, Izmaylov AF, Bloino J, Zheng G, Sonnenberg JL, Hada M, Ehara M, Toyota K, Fukuda R, Hasegawa J, Ishida M, Nakajima T, Honda Y, Kitao O, Nakai H, Vreven T, Montgomery JA, Peralta JE, Ogliaro F, Bearpark M, Heyd JJ, Brothers E, Kudin KN, Staroverov VN, Kobayashi R, Normand J, Raghavachari K, Rendell A, Burant JC, Iyengar SS, Tomasi J, Cossi M, Rega N, Millam JM, Klene M, Knox JE, Cross JB, Bakken V, Adamo C, Jaramillo J, Gomperts R, Stratmann RE, Yazyev O, Austin AJ, Cammi R, Pomelli C, Ochterski JW, Martin RL, Morokuma K, Zakrzewski VG, Voth GA, Salvador P, Dannenberg JJ, Dapprich S, Daniels AD, Farkas O,

- Foresman JB, Ortiz JV, Cioslowski J, Fox DJ, GAUSSIAN 09, Revision A.02, Gaussian Inc, Wallingford CT, 2009.
11. Frisch A, Nielson AB, Holder AJ, Gaussview user manual, Gaussian Inc., Pittsburgh, PA, 2009.
 12. MOLVIB (V.7.0): Calculation of Harmonic Force Fields and Vibrational Modes of Molecules, QCPE Program No. 807, 2002.
 13. Gomes LR, Nicolson Low J, Cagide F, Gaspar A and Borges F, A comparison of the structures of some 2- and 3-substituted chromone derivatives: a structural study on the importance of the secondary carboxamide backbone for the inhibitory activity of MAO-B, *Acta Cryst.*, E71, 2015, 1270–1277.
 14. Young DC, *Computational Chemistry: A Practical Guide for Applying Techniques to Real-World Problems*, John Wiley & Sons Inc., New York, 2001.
 15. Senthil Kumar J, Jeyavijayan S, Arivazhagan M, Spectroscopic (FT-IR and FT-Raman) investigation, first order hyperpolarizability, NBO, HOMO–LUMO and MEP analysis of 6-nitrochromone by ab initio and density functional theory calculations, *Spectrochim. Acta* 136A, 2015, 771-781.
 16. Jeyavijayan S, Gobinath E, Senthil Kumar J, Structural, Spectroscopic Investigation and Quantum Chemical Calculation Studies of 2,4,6-trimethylphenol for Pharmaceutical Application, *Int. J. Pharm. Sci. Rev. Res.*, 41, 2016, 214-222.
 17. Arivazhagan M, Manivel S, Jeyavijayan S, Meenakshi R, Vibrational spectroscopic (FTIR and FT-Raman), first-order hyperpolarizability, HOMO, LUMO, NBO, Mulliken charge analyses of 2-ethylimidazole based on Hartree–Fock and DFT calculations *Spectrochim. Acta* 134A, 2015, 493–501.
 18. David Suresh Babu P, Periandy S, Ramalingam S, Vibrational spectroscopic (FTIR and FTRaman) investigation using ab initio (HF) and DFT (LSDA and B3LYP) analysis on the structure of Toluic acid, *Spectrochim. Acta* 78A, 2011, 1321-1328.
 19. Sert Y, El-Emam AA, Al-Deeb OA, Al-Turkistani AA, Uzun F, Cirak C, The biomolecule, 2-[(2-methoxy)sulfanyl]-4-(2-methylpropyl)-6-oxo-1,6-dihydropyrimidine-5-carbonitrile: FT-IR, Laser-Raman spectra and DFT, *Spectrochim. Acta* 126A, 2014, 86–97.
 20. Socrates G, *Infrared and Raman Characteristic Group Frequencies – Tables and Charts*, third ed., Wiley, Chichester, 2001.
 21. Fleming I, *Frontier Orbitals and Organic Chemical Reactions*, Wiley, London, 1976.
 22. Mulliken RS, Electronic Population Analysis on LCAO-MO Molecular Wave Functions, *J. Chem. Phys.* 23, 1955, 1833-1840.
 23. Murray JS, Sen K, *Molecular Electrostatic Potentials, Concepts and Applications*, Elsevier, Amsterdam, 1996, pp. 7–624.
 24. D.A. Kleinman, Nonlinear Dielectric Polarization in Optical Media, *Phys. Rev.* 126, 1962, 1977-1979.
 25. Sun YX, Hao QL, Wei WX, Yu ZX, Lu LD, Wang X, Wang YS, Experimental and density functional studies on 4-(3,4-dihydroxybenzylideneamino)antipyrene, and 4-(2,3,4-trihydroxybenzylideneamino)antipyrene, *J. Mol. Struct. (Theochem.)* 904, 2009, 74-82.

Source of Support: Nil, Conflict of Interest: None.

